DOI: 10.1002/chem.200901582

Ir^{III} and Ru^{II} Complexes Containing Triazole-Pyridine Ligands: Luminescence Enhancement upon Substitution with β-Cyclodextrin

Marco Felici,[a] Pablo Contreras-Carballada,[b] Yolanda Vida,[c, d] Jan M. M. Smits,[e]
Roeland J. M. Nolte,[a] Luisa De Cola,*[c] René M. Williams,*[b] and Martin C. Feiters*[a]

Abstract: Novel 2-(1-substituted-1*H*-1,2,3-triazol-4-yl)pyridine (pytl) ligands have been prepared by "click chemistry" and used in the preparation of heteroleptic complexes of Ru and Ir with bipyridine (bpy) and phenylpyridine (ppy) ligands, respectively, resulting in $[Ru(bpy)_2(pytl\text{-}R)]Cl_2$ and $[Ir(ppy)_2(pytl\text{-}R)]Cl$ (R = methyl, adamantane (ada), β-cyclodextrin (βCD)). The two diastereoisomers of the Ir complex with the appended β-cyclodextrin, $[Ir(ppy)_2(pytl\text{-}\beta CD)]Cl$, were separated. The $[Ru(bpy)_2(pytl\text{-}R)]Cl_2$ (R = Me, ada or βCD) complexes have lower lifetimes and quantum yields than other polypyridine complexes. In contrast, the cyclometalated Ir complexes display rather long lifetimes and very high emission quantum yields. The emission quantum yield and lifetime ($\Phi = 0.23$, $\tau = 1000$ ns) of $[Ir(ppy)_2(pytl\text{-}ada)]Cl$ are surprisingly enhanced in $[Ir(ppy)_2(pytl\text{-}\beta CD)]Cl$ ($\Phi = 0.54$, $\tau = 2800$ ns). This behavior is unprecedented for a metal complex and is most likely due to its increased rigidity and protection from water molecules as well as from dioxygen quenching, because of the hydrophobic cavity of the βCD covalently attached to pytl. The emissive excited state is localized on these cyclometalating ligands, as underlined by the shift to the blue (450 nm) upon substitution with two electron-withdrawing fluorine substituents on the phenyl unit. The significant differences between the quantum yields of the two separate diastereoisomers of $[Ir(ppy)_2(pytl\text{-}\beta CD)]Cl$ (0.49 vs. 0.70) are attributed to different interactions of the chiral cyclodextrin substituent with the Δ and Λ isomers of the metal complex.

Keywords: click chemistry · cyclodextrins · iridium · luminescence · ruthenium

---

[a] M. Felici, Prof. Dr. R. J. M. Nolte, Dr. M. C. Feiters
Department of Organic Chemistry
Institute for Molecules and Materials
Radboud University Nijmegen, Heijendaalseweg 135
6525 AJ Nijmegen (The Netherlands)
Fax: (+31) 243-652-929
E-mail: m.feiters@science.ru.nl

[b] Dr. P. Contreras-Carballada, Dr. R. M. Williams
Molecular Photonic Materials
Van't Hoff Institute for Molecular Sciences
Universiteit van Amsterdam, Nieuwe Achtergracht 129
1018 WS Amsterdam (The Netherlands)
Fax: (+31) 205-256-456
E-mail: R.M.Williams@uva.nl

[c] Dr. Y. Vida, Prof. Dr. L. De Cola
Physikalisches Institut and CeNTech
Westfälische Wilhelms-Universität Münster
Mendelstrasse 7, 48149 Münster (Germany)
Fax: (+49) 251-980-2834
E-mail: decola@uni-muenster.de

[d] Dr. Y. Vida
Present address: Department of Organic Chemistry
Faculty of Sciences
University of Malaga, 29071 Malaga (Spain)

[e] J. M. M. Smits
Solid State Chemistry, Institute for Molecules and Materials
Radboud University Nijmegen, Heijendaalseweg 135
6525 AJ Nijmegen (The Netherlands)

Supporting information for this article (synthesis and characterization of the compounds; HPLC chromatograms; transient absorption spectra of some compounds; tables of crystal data and structure refinement, selected bond distances and angles, coordinates and anisotropies, and PLATON plots for crystal structures; estimated quenching constants for molecular oxygen; a color version of Figure 5) is available on the WWW under http://dx.doi.org/10.1002/chem.200901582.

Introduction

Cu-catalyzed dipolar [3+2] cycloaddition, better known as the "click reaction",[1] involves the efficient formation of 1,2,3-triazole rings by coupling terminal alkynes and azides, and can be used to synthesize a bidentate triazole-pyridine ligand, 2-(1-substituted-1*H*-1,2,3-triazol-4-yl)pyridine (pytl; see Scheme 1).[2,3] This novel approach is extremely flexible; it allows in principle for the functionalization of any azide-appended molecule with this ligand, as has been shown for 4-butoxyphenylazide[4] as well as for relatively small[5] and large carbohydrates, such as cyclodextrins.[6]

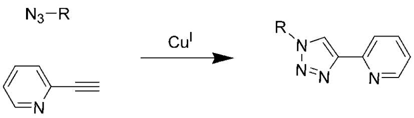

Scheme 1. Preparation of pytl by the Cu-catalyzed Huisgen dipolar [3+2] cycloaddition.

Cyclodextrins (CDs) are well-known cyclic oligosaccharides that can form inclusion complexes in aqueous solution with a variety of hydrophobic substrates, such as adamantane derivatives, and have been widely applied as supramolecular building blocks in various areas,[7–13] including photoactivated electron transfer processes.[14–19] By applying click chemistry to 2-ethynylpyridine and monoazido βCD the cyclodextrin-appended triazole-pyridine (pytl-βCD, **1**) could be readily prepared[20] and complexed with metal ions. Complexes of Ru[21–26] and especially of Ir[27–34] have received increasing attention in recent years because of their promising photophysical properties; they have been described as efficient photosensitizers, applied in the manufacture of optical devices (in solution and in the solid state), and as components for organic light-emitting diodes (OLEDs). Because of our interest in such properties,[14–17] we prepared and characterized a series of heteroleptic octahedral complexes containing one substituted triazole-pyridine ligand. Here we report the synthesis and the photophysical properties of such complexes of **1** with Ru^{II} and Ir^{III}, in which the coordination sphere is completed by bipyridine (bpy) for Ru^{II} and phenylpyridine (ppy) for Ir^{III}, giving the complexes $[Ru(bpy)_2(pytl\text{-}\beta CD)]Cl_2$ and $[Ir(ppy)_2(pytl\text{-}\beta CD)]Cl$, respectively.

By applying click chemistry to azide-appended adamantane and 2-ethynylpyridine, we also prepared 2-(1-adamantyl-1*H*-1,2,3-triazol-4-yl)pyridine (pytl-ada, **2**) and its Ru and Ir complexes $[Ru(bpy)_2(\mathbf{2})]Cl_2$ and $[Ir(ppy)_2(\mathbf{2})]Cl$. Starting from methyl azide, pytl-Me **3** was prepared, together with its Ru complex $[Ru(bpy)_2(\mathbf{3})]Cl_2$.

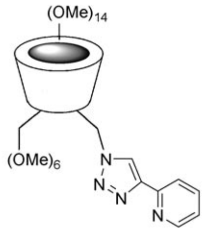

1

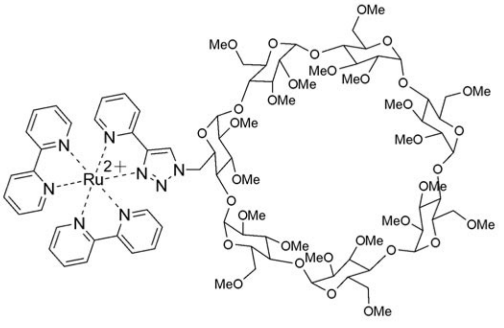

$[Ru(bpy)_2(\mathbf{1})]Cl_2$

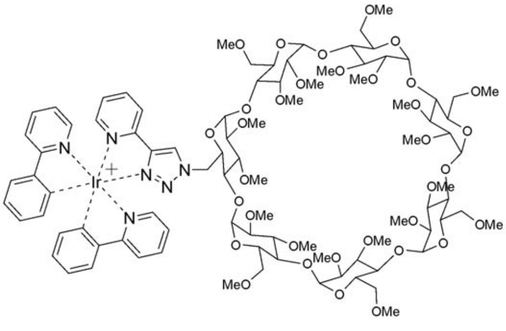

$[Ir(ppy)_2(\mathbf{1})]Cl$

Several approaches to tuning the emission energy of cyclometalated Ir complexes have focused on decreasing the HOMO energy while keeping the LUMO energy relatively unchanged. The addition of electron-withdrawing groups to the phenyl ring has been used as one way to achieve this goal. The most common withdrawing group used for this

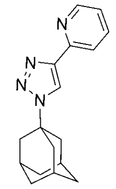

2

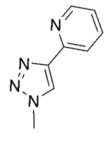

3

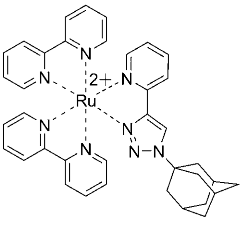

$[Ru(bpy)_2(\mathbf{2})]Cl_2$

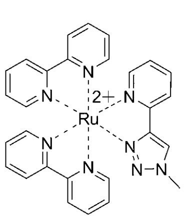

$[Ru(bpy)_2(\mathbf{3})]Cl_2$

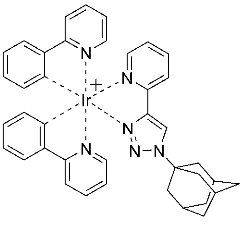

$[Ir(ppy)_2(\mathbf{2})]Cl$

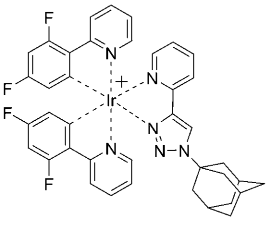

$[Ir(F_2ppy)_2(\mathbf{2})]Cl$

purpose is fluorine.[34,35] For this reason, we prepared complexes of **2** in which the coordination sphere of Ir was completed either with ppy or its 3,5-bisfluorinated analogue F_2ppy.

There are some examples in the literature of ruthenium complexes containing 1,2,3-triazole ligands.[36–39] Ru complexes in which the coordination sphere is occupied by one or three pytl ligands have been described but emission properties have never been reported.[36,37] Some examples of analogues of ruthenium bisterpyridine have also been mentioned, in which each terpyridine ligand has been substituted for a 2,6-bis(1-methyl-1*H*-1,2,3-triazol-4-yl)pyridine ligand.[38,39] The preparation of Ir complexes containing triazole-pyridine ligands has been published recently.[40] However, these ligands differ from ours because they do not have a substituent on the nitrogen in position 1, they are negatively charged, and the corresponding iridium complexes are neutral. The functionalization of Ir complexes with βCD has never been described. An obvious advantage of the monofunctionalization of βCD with pytl over the functionalization of all the primary hydroxyls of this compound described earlier[6] is that it enables studies on a single metal ion bound to a cyclodextrin molecule. On the other hand, it is responsible for the loss of symmetry in the cyclodextrin moiety, thus leading to rather complex NMR spectra. For this reason, high-resolution NMR spectroscopy techniques were applied for the characterization of these derivatives.

In this paper we show that the cyclometalated Ir complexes $[Ir(ppy)_2(pytl\text{-}R)]Cl$ (R = ada or βCD) containing 1-substituted pytl ligands display blue-greenish emission possessing the characteristic long triplet lifetimes and surprisingly high emission quantum yields, especially for the βCD derivative, $[Ir(ppy)_2(\mathbf{1})]Cl$. By HPLC separation, NMR spectroscopy, circular dichroism, and X-ray crystallographic studies we established that the complex $[Ir(ppy)_2(\mathbf{1})]Cl$ exists in two diastereoisomeric forms. These diastereoisomers show an unexpectedly large difference in their quantum yields, considering the fact that the metal centers are in an enantiomeric relationship. To our knowledge such behavior has never been reported previously for metal complexes; it is due to a noncovalent interaction of the Ir complex with the covalently attached βCD, which acts as a chiral second-sphere ligand.

Results and Discussion

Synthesis of pytl ligands and their Ru and Ir complexes: The established high efficiency and versatility of the click reaction[1] (Scheme 1) is the key to the success of our approach. A small library of differently functionalized ligands was very easily prepared, starting from three different molecules all containing an azide, simply by carrying out the click reaction in the presence of 2-ethynylpyridine. In the case of the monofunctionalized βCD it was further decided to methylate the 20 remaining hydroxyl groups, thus making the molecule soluble in a wider range of solvents[41] as well as easier to purify by chromatography,[41] and extending the hydrophobic cavity so that its binding properties would be improved.[7] The preparation of the permethylated mono-pytl-appended βCD **1** from βCD **4** (Scheme 2) proceeded via the monotosyl-βCD derivative **4a**, the monoazido βCD **4b**, and the monoazido permethylated βCD **5** as described elsewhere.[42] Compound **5** was then reacted with 2-ethynylpyridine **6** in deoxygenated THF, in the presence of CuBr

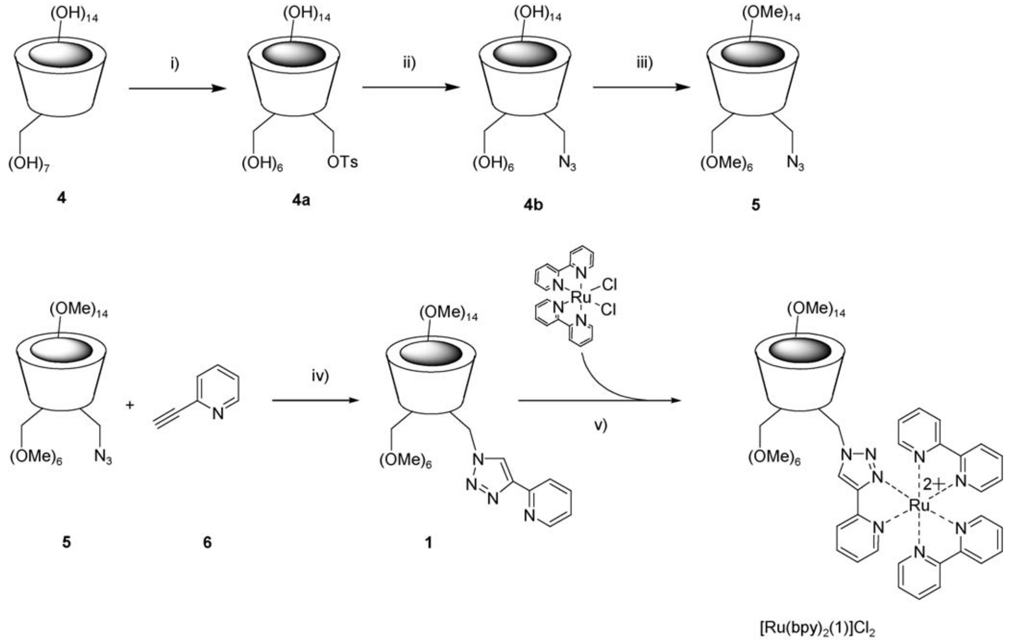

Scheme 2. Synthesis of **5** and $[Ru(bpy)_2(\mathbf{1})]Cl_2$. Reagents and conditions: i) H_2O, NaOH, TsCl; ii) DMF, NaN_3, 60 °C; iii) DMF, NaH, CH_3I; iv) CuBr, PMDTA, THF, under N_2, 2 h; v) mixture of 5 % water in 2-methoxyethanol, 90 °C, 24 h.

and pentamethyldiethylenetriamine (PMDTA). This reaction is extremely selective and efficient, leading to the desired compound **1** in 91% yield without any side products. The novel ligands pytl-ada **2** and pytl-Me **3** were prepared analogously, by reaction of **6** with 1-azidoadamantane and methyl azide, respectively. The complex $[Ru(bpy)_2(\mathbf{1})]Cl_2$ was prepared by reaction of the pytl ligand **1** with the commercially available *cis*-$Ru(bpy)_2Cl_2$ for 24 h (Scheme 2) to give, in 92% yield, an orange solid which, after purification by HPLC, was found to correspond to the desired structure. The complexes $[Ru(bpy)_2(R)]Cl_2$ ($R = \mathbf{2}, \mathbf{3}$) were prepared by following an analogous synthetic path. The compounds $[Ir(ppy)_2(X)]Cl$ ($X = \mathbf{1}, \mathbf{2}$) and $[Ir(F_2ppy)_2(\mathbf{2})]Cl$ were synthesized easily by replacing the bridging chlorides from the Ir^{III} μ-chloro-bridged dimer $(ppy)_2Ir(\mu\text{-}Cl)_2Ir(ppy)_2$ with the corresponding bidentate pytl ligands. The mono-pytl βCD **1** reacted with the dinuclear species under quite mild conditions, in chloroform/methanol (3:1, v/v) at 45 °C (Scheme 3). After 3 h the formation of only one new spot was observed in the TLC, characterized (in contrast to the starting compound **1**) by an extremely bright green luminescence under a UV/Vis lamp at 366 nm. $[Ir(ppy)_2(\mathbf{2})]Cl$ and $[Ir(F_2ppy)_2(\mathbf{2})]Cl$ were prepared analogously. In all cases the purification was performed by silica-gel chromatography or by HPLC on a reversed-phase column (see the Experimental Section) to give yellow solids in high yields (91–95%).

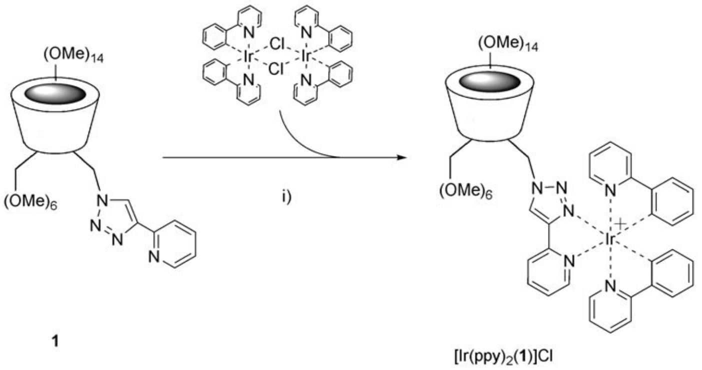

Scheme 3. Synthesis of $[Ir(ppy)_2(\mathbf{1})]Cl$. Conditions: i) chloroform/methanol, 3:1 (v/v), 45 °C, 3 h.

The structures of the two ligands (**2**, pytl-ada; **3**, pytl-Me) and of the Ir complex ($[Ir(ppy)_2(\mathbf{2})]Cl$ were determined by crystallography; details are given in Table S1, structures in Figures S1–S3, selected bond distances and angles in Tables S2–S4, and atomic coordinates and equivalent isotropic displacement parameters in Tables S5–S7. The packing of the molecules of the enantiomers of $[Ir(ppy)_2(\mathbf{2})]Cl$ will be discussed in the section on the structural characterization of $[Ir(ppy)_2(\mathbf{1})]Cl$ (see below).

Photophysical characterization

Absorption and emission of Ru and Ir complexes: The photophysical properties of the iridium and ruthenium pytl complexes were determined by steady-state and time-resolved spectroscopic methods. The absorption spectra of all Ru and Ir complexes in water at room temperature (Figure 1) show intense bands in the UV region (290 nm) and moderately intense bands in the visible region (350–500 nm) that are typical for ruthenium and iridium polypyridyl complexes. All the bands can be interpreted by comparing the absorption spectra of the ruthenium complexes (Figure 1, top) with that assigned to $Ru(bpy)_3^{2+}$.[26] The bands at wavelengths shorter than 300 nm belong to the allowed π–π* transitions of the coordinated ligands and in particular to the bipyridine units, and the shoulder that appears at 280 nm is due to the substitution of one of the pyridine rings by the triazole ring. All the complexes display the typical metal-to-ligand charge-transfer singlet (^{1}MLCT) band between 400 and 500 nm; whereas $Ru(bpy)_3^{2+}$ shows a clear maximum at 452 nm, in our complexes the coexistence of different ligands at similar energies leads to a set of MLCT bands due to the transitions from the metal to the bpy ligands or to the triazole-pyridine ligand.

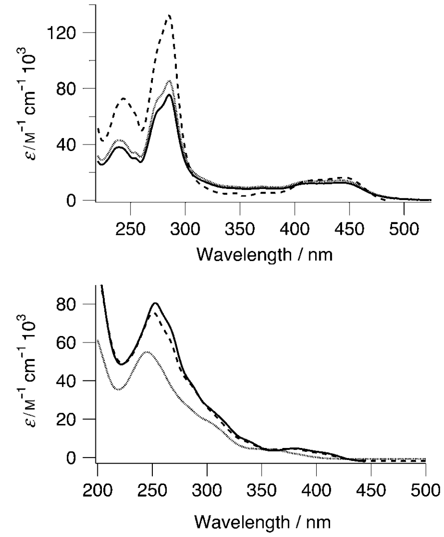

Figure 1. UV/Vis absorption spectra of Ru complexes (top; ——, $[Ru(bpy)_2(\mathbf{1})]Cl_2$; •••••, $[Ru(bpy)_2(\mathbf{2})]Cl_2$; -----, $[Ru(bpy)_2(\mathbf{3})]Cl_2$) and Ir complexes (bottom; ——, $[Ir(ppy)_2(\mathbf{2})]Cl$; -----, $[Ir(ppy)_2(\mathbf{1})]Cl$; •••••, $[Ir(F_2ppy)_2(\mathbf{2})]Cl$) in water.

For the iridium complexes (Figure 1, bottom) the absorption spectra resemble those of triazole Ir complexes.[40,43] The bands in the 250–300 nm region belong again to the allowed intraligand π–π* transitions of the phenyl-pyridine units and of the triazole-pyridine. The absorption spectra of the iridium complexes show ^{1}MLCT transitions at energies lower than the ligand π–π* transitions, in the 300–350 nm region, partially overlapping with the spin-forbidden ^{3}MLCT transitions, which extend to 400 nm.[34,44]

The luminescence spectra of the ruthenium complexes (Figure 2, top) show a broad band centered around 610 nm and typical of the radiative decay from a ^{3}MLCT state. In the case of the iridium complexes (Figure 2, bottom) with

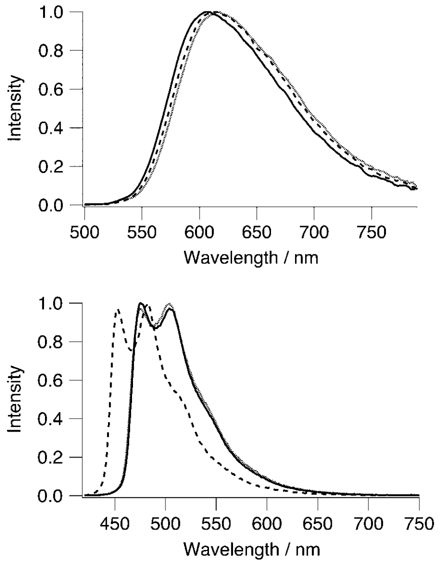

Figure 2. Room-temperature emission spectra in water of Ru complexes (top; $\lambda_{exc}=445$ nm; ——, $[Ru(bpy)_2(\mathbf{1})]Cl_2$; •••••, $[Ru(bpy)_2(\mathbf{2})]Cl_2$; -----, $[Ru(bpy)_2(\mathbf{3})]Cl_2$) and Ir complexes (bottom; $\lambda_{exc}=380$ nm; ——, $[Ir(ppy)_2(\mathbf{1})]Cl$; •••••, $[Ir(ppy)_2(\mathbf{2})]Cl$; -----, $[Ir(F_2ppy)_2(\mathbf{2})]Cl$).

Table 1. Luminescence lifetimes and emission quantum yields of the complexes.

Complex[a]	λ_{em}[nm][b]	Φ(air)[b,d]	Φ(Ar)[b,e]	τ(air) [ns][c,d]	τ(Ar) [ns][c,e]	τ(77 K) [ns][f]
$[Ru(bpy)_2(\mathbf{1})]Cl_2$	610	0.0054	0.0056	24.0	24.8	6300
$[Ru(bpy)_2(\mathbf{2})]Cl_2$	615	0.0047	0.0048	19.1	19.6	6000
$[Ru(bpy)_2(\mathbf{3})]Cl_2$	615	0.0060	0.0062	26.3	27.4	6000
$[Ir(ppy)_2(\mathbf{1})]Cl$	475	0.14	0.54	690	2800	5300
$[Ir(ppy)_2(\mathbf{2})]Cl$	475	0.076	0.23	435	1000	5200
$[Ir(F_2ppy)_2(\mathbf{2})]Cl$	450	0.071	0.16	480	1100	6000

[a] **1** = pytl-βCD, **2** = pytl-ada, **3** = pytl-Me. [b] Ruthenium was excited at 448 nm and iridium at 402 nm. [c] Ruthenium was excited at 420 nm and iridium at 380 nm. [d] The solutions were measured in air-equilibrated water. [e] The solutions were measured in argon-saturated water degassed by bubbling argon through the solutions for 20–30 min. [f] The glassy EtOH/MeOH (1:1) matrix samples were excited at 435 nm.

the phenyl-pyridine ligands and the substituted triazole-pyridine we can see the resolved vibronic structure typical of this type of complex. The lowest excited state for Ir is also a ^{3}MLCT state, but for such high-energy-emitting complexes a certain degree of mixing with the ligand-centered triplet (^{3}LC) is present. Fluorination of the phenyl rings on the ppy ligands lowers the energy of the HOMO orbital in the molecules. The lowering of the LUMO energy is significantly less than for the HOMO, resulting in a widening of the HOMO–LUMO gap and leading to an increase in excited-state energy. This is translated into a blue shift in the emission on going from the green emitters (nonfluorinated) to the blue emitters (fluorinated complexes) (Figure 2, bottom). In the homoleptic complexes $Ir(ppy)_3$ and the fluorinated homologue $Ir(F_2ppy)_3$ a blue shift of 39 nm occurs.[45] The quantum yields of emission as well as the emission lifetimes for both Ru and Ir complexes were determined in aqueous solutions under air-equilibrated and in deaerated conditions (Table 1). The pytl ligand appears to influence the excited states of the ruthenium and iridium complexes in different ways.

Ruthenium complexes exhibit rather short lifetimes and low quantum yields[46] and their photophysical properties are therefore unaffected by the presence of dioxygen (Table 1).

The lowest excited state most likely involves the bipyridine ligands because the LUMO of the triazole is more electron-rich and therefore higher in energy than those of the pyridines. In ruthenium complexes containing 1,2,4-triazole-pyridine ligands, the lowest-energy excited electronic states are predominantly bipyridine-based.[46–50] We believe that in our case also we have the same trend, but that this is affected by the nitrogen substitution of the triazole, which renders the substituted triazole a worse σ donor than the unsubstituted 1,2,4-triazole. As a consequence we would expect a smaller ligand field for the triazole-pyridine, which would cause a lowering of the metal-centered triplet states (^{3}MC), which are known to be thermally populated and efficient nonradiative channels for the depopulation of the luminescent ^{3}MLCT state.[51] A similar behavior is also observed upon protonation of the nitrogen in position 4 in ruthenium complexes with a 1,2,4-triazole-pyridine ligand. Such electronic properties are reflected in the poor emitting properties of our complexes.

A different situation is observed with the compounds which display excited-state lifetimes in the microsecond range typical of cyclometalated iridium complexes;[29,32] they all decay with monoexponential kinetics. They also show high emission quantum yields. Due to the long lifetime of their excited states, which is related to the triplet character of the emission, they are very sensitive to dioxygen, which can therefore quench their luminescent excited states. In general, the emission energies of luminescent cyclometalated iridium complexes are strongly influenced by the triplet energy of the ligand.[52,53] The HOMO is composed principally of p orbitals of the phenyl ring and metal d orbitals of the Ir. The pyridine is more electronegative and is therefore responsible for the LUMO. In many cases and in particular for blue emitters, the lowest excited state of the complex is best described as an admixture of ^{3}LC and ^{3}MLCT states.[45,54–56]

Very interestingly, the substitution with a β-cyclodextrin alters the photophysical behavior greatly compared with the adamantyl derivative. Even though the emission maximum is unchanged, indicating the same nature and involvement of the coordinated ligand, the emission quantum yields, for both air-equilibrated and deaerated water solutions, increase dramatically (Φ(air) = 0.14, Φ(Ar) = 0.54). The excited state lifetimes also change and in particular become longer (see Table 1). Such an elongation of the air-equilibrated lifetime points to a shielding of the emitting core from dioxygen. This is perhaps caused by the βCD, which could in some way interact with the phenyl-pyridine ligands, partially keeping the water and the oxygen away from the Ir core. Such effects on phosphorescent molecules inside cyclodextrin complexes have been observed previously.[13,18,19,57] The permethylated cyclodextrin has a very flexible structure compared to the native CD, due to the breaking of its internal hydrogen bonds. The primary side of the cavity is very close to the metal center and, due to its flexibility, it could approach the complex, partially shielding the ligands involved in the lowest excited states, with a consequent reduction of nonradiative decay processes. An estimate of the quenching constant k_q that describes the quenching of the Ir complexes by molecular oxygen can be obtained by applying the Stern–Volmer equation to the ratios of the quantum yields and the lifetimes given in Tables 1 and 2 (see below) and is included in the Supporting Information. The formation of singlet oxygen by using photosensitizers is well known and has also been discussed recently for iridium complexes,[58] but it was not investigated for our complexes.

Low-temperature luminescence: Comparison of Figure 3, which shows the low-temperature luminescence emission of the ruthenium and iridium complexes at 77 K in a EtOH/MeOH glassy matrix, with the spectra at room temperature (Figure 2) reveals that the emission spectra become well structured for the iridium and the ruthenium compounds in the low-temperature experiments. [Ir(ppy)$_2$(**1**)]Cl and [Ir(ppy)$_2$(**2**)]Cl have spectra that nearly overlap in peak position and relative peak intensities. As expected, a difference arises with the fluorinated complex [Ir(F$_2$ppy)$_2$(**2**)]Cl, which shows a blue shift in the emission. All three emission spectra of the ruthenium compounds are clearly very similar with only a minor difference in the emission of [Ru(bpy)$_2$(**3**)]Cl$_2$ in the higher-wavelength region.

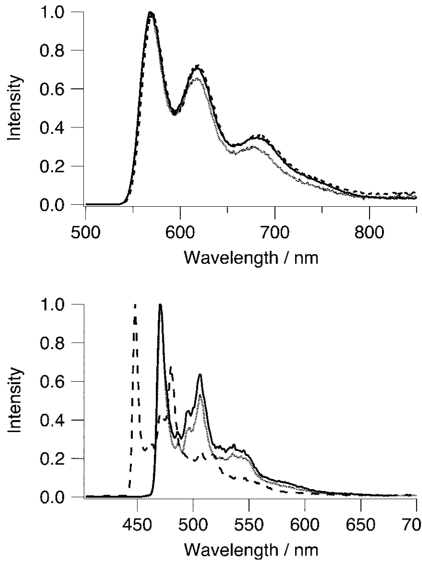

Figure 3. 77 K luminescence spectra in a glassy EtOH/MeOH (1:1) matrix of ruthenium complexes (top; λ_{exc} = 445 nm, ——, [Ru(bpy)$_2$(**1**)]Cl$_2$; •••••, [Ru(bpy)$_2$(**2**)]Cl$_2$; -----, [Ru(bpy)$_2$(**3**)]Cl$_2$) and iridium compounds (bottom; λ_{exc} = 380 nm; ——, [Ir(ppy)$_2$(**1**)]Cl; •••••, [Ir(ppy)$_2$(**2**)]Cl; -----, [Ir(F$_2$ppy)$_2$(**2**)]Cl).

The vibronic structure of the iridium complexes corresponds to 1200 cm^{-1}, the ring-vibration frequency of the phenyl-pyridine ligand, confirming the participation of the ligand in the emission.[59]

For the ruthenium complexes the vibronic structure corresponds to 1400 and 1500 cm^{-1}, the ring-breathing frequencies of the bipyridine ligand, confirming the participation of this ligand in the excited-state luminescence emission of the complex as well.[60] This corroborates the assumption made above that the lowest emitting state involves the bipyridine ligands and that the triazole has little or no influence on the energy of the emissive state. The emission maximum is blue-shifted (relative to room temperature), as expected for charge transfer states and already observed for bipyridine complexes.[26]

Transient absorption measurements of the complexes: As discussed above, the excited-state properties of the iridium complexes can be described by an admixture of ^{3}LC and ^{3}MLCT states. Transient absorption spectra were recorded to investigate further the exact nature of the excited state in air-equilibrated water at room temperature. The complex [Ir(ppy)$_2$(**1**)]Cl (Figure 4) presents two absorption bands, at 360 and 450 nm; the same spectrum is observed for [Ir(ppy)$_2$(**2**)]Cl (Figure S4). Both bands decay monoexponentially with similar lifetimes to those observed with time-resolved emission, suggesting that the emissive and absorbing states are identical. A similar behavior is observed for [Ir(F$_2$ppy)$_2$(**2**)]Cl (Figure S5); however, in this case the transient is formed by only one band, which is less well defined, between 300 and 500 nm with a maximum at 380 nm. All

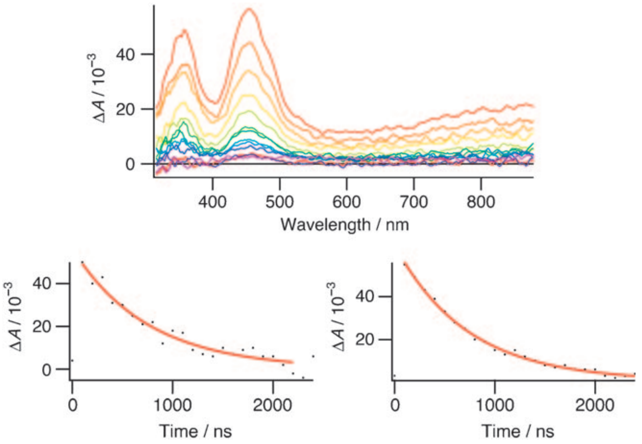

Figure 4. Top: Transient absorption spectrum of [Ir(ppy)$_2$(**1**)]Cl after laser light excitation at λ = 380 nm, with decay kinetics at λ = 360 nm (bottom left) and λ = 449 nm (bottom right). 250 accumulations per frame, 25 frames (only first and odd numbered frames are shown in the transient spectrum for clarity), 100 ns increment in between frames. Decay at λ = 360 nm, τ = 754 ns. Decay at λ = 449 nm, τ = 723 ns.

the transient spectra for these complexes show an absorption band tailing into the infrared.

For the orthometalated complex $Ir(ppy)_3$ the transient spectrum characterized by a band centered at 370 nm with a shoulder around 480 nm and a featureless tail extending to the near-infrared region has been reported.[61] In our case similar bands appear,[62] which could therefore be ascribed to an excited state localized on the ppy ligands, with an MLCT character and the lower-energy bands tentatively assigned to T_1–T_n transitions. In the case of $[Ir(F_2ppy)_2(\mathbf{2})]Cl$ the presence of the fluorine atoms that lower the HOMO level, and the higher degree of mixing between the MLCT and LC states, result in a featureless broad band (Figure S5).

The transient absorption spectra of the ruthenium complexes were recorded in argon-saturated water (degassed conditions) to obtain more insight into the nature of the excited states. In all three cases the spectra are very similar, indicating that the substituents attached to the triazole do not induce significant changes in the excited-state absorption properties (Figure S6). The transient absorption spectrum of $Ru(bpy)_3^{2+}$ is very well known and the comparison with our systems can be very useful in assigning the observed bands.[63] Transient absorption spectra show a strong bleaching of ground-state absorption upon excitation, with a recovery comparable with that obtained from emission lifetime measurements (between 25 and 30 ns) (Figure S6). All the complexes studied show a strong excited-state peak at about 380 nm that has been identified as due to the radical anion ($bpy^{\bullet -}$) absorption, confirming the assignment of an MLCT involving the bpy as the lowest excited state.

Structural characterization of $[Ir(ppy)_2(\mathbf{1})]Cl$ diastereoisomers: The iridium complexes $[Ir(ppy)_2(L)Cl]$ (L = ligand) are always prepared by reaction of an ancillary ligand with the Ir^{III} μ-chloro-bridged dimer $(ppy)_2Ir(\mu\text{-}Cl)_2Ir(ppy)_2$ (*mer* configuration) in which the nitrogen atoms of the ppy ligands are always in a *trans* position with respect to the metal atom.[64] This fact limits the number of possible stereoisomers of the resulting complexes that coordinate three bidentate ligands (two ppy, one pytl) to one pair of enantiomers. Our $[Ir(ppy)_2(\mathbf{2})]Cl$ crystals proved to be a racemic mixture (Figure 5), containing two pairs of enantiomers (Δ and Λ) in each unit cell ($Z = 4$).

The covalent functionalization of a metal complex that exists in two enantiomeric forms with the chiral enantiopure βCD, composed of α-D-glucose building blocks, leads to the formation of diastereoisomeric species (Figure 6a,b). As the geometry of metal complexes can play an important role in photophysics, we investigated the effects of the existence of two diastereoisomers of $[Ir(ppy)_2(\mathbf{1})]Cl$ in more detail.

The native βCD has a *C*7 symmetry that is broken by the monofunctionalization, and this fact is responsible for the high complexity of the carbohydrate region of the ^1H NMR spectra. The situation becomes even more complex in the case of $[Ir(ppy)_2(\mathbf{1})]Cl$ because the two diastereoisomers are expected to display different NMR spectra. Indeed, the

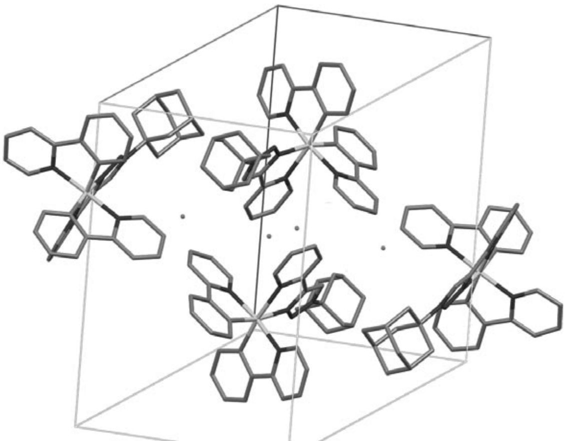

Figure 5. Unit cell of $[Ir(ppy)_2(\mathbf{2})]Cl$. The top and bottom structures toward the left are Δ; the top and bottom ones toward the right are Λ. Hydrogen atoms and solvent (H_2O) molecules are omitted for clarity.

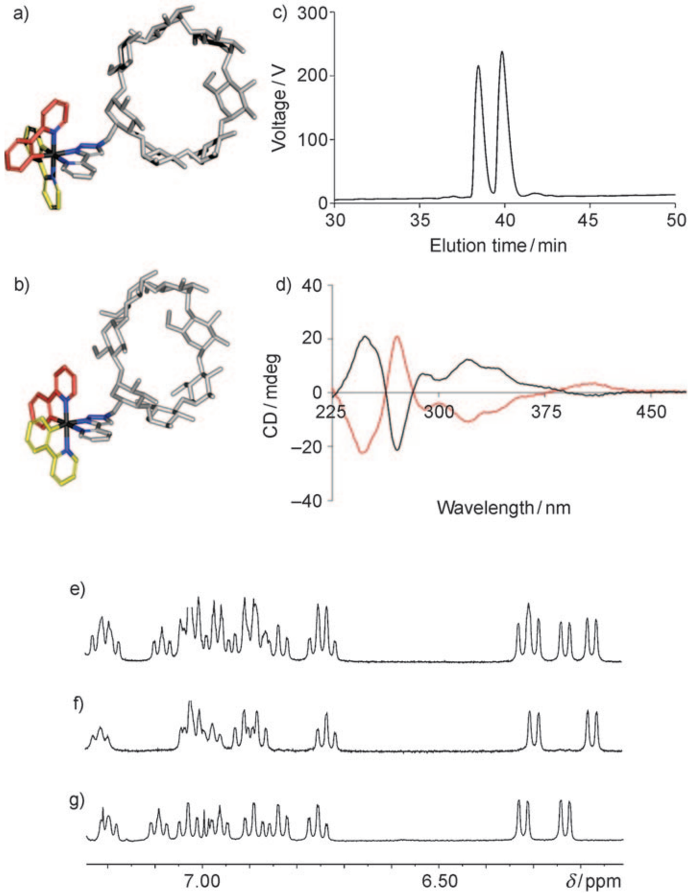

Figure 6. a) Δ and b) Λ diastereoisomeric forms of $[Ir(ppy)_2(\mathbf{1})]Cl$; c) HPLC chromatogram: separation of the two Ir complexes by using a gradient of acetonitrile and H_2O containing 0.1 % v/v HCl. d) Circular dichroism spectra in H_2O of HPLC fractions: red, 1st HPLC peak; black, 2nd HPLC peak. e–g) Part of the aromatic region of the ^1H NMR spectra of e) the mixture of diastereoisomers of $[Ir(ppy)_2(\mathbf{1})]Cl$; f) the 1st fraction corresponding to **A**, g) the 2nd fraction corresponding to **B** (400 MHz, $CDCl_3$, 25 °C).

^{1}H NMR spectrum of the mixture of [Ir(ppy)$_2$(**1**)]Cl (Figure 6e) suggests the presence of two different compounds in a 44:56 ratio. We found that these diastereoisomers can be separated on an achiral reversed-phase HPLC column with 0.1 % (v/v) HCl or TFA in the mobile phase (Figure 6c); the ratio calculated from the peak areas corresponds to that derived from NMR. Under the same conditions in a semipreparative HPLC column, the two isomeric compounds were isolated in milligram scale, fully characterized, and labeled [Ir(ppy)$_2$(**1**)]Cl(**A**) and (**B**) in order of elution.

In the aromatic region of the ^{1}H NMR spectra in Figure 2e–g, the spectrum of the mixture of [Ir(ppy)$_2$(**1**)]Cl can be reproduced perfectly by overlapping the spectra of the two isolated isomers (**A**) and (**B**). The suggestion that these compounds are identical in the configuration of the cyclodextrin moiety, but have different arrangements of the bidentate ligands around the metal (Figure 6a,b), was further corroborated by their circular dichroism spectra (Figure 6d): the two isomers have identical absorption spectra with ellipticities of opposite sign. Comparison with circular dichroism spectra of enantiomerically pure cyclometalated Ir complexes from the literature[65] allows assignment of the first peak (**A**) as the Δ and the second (**B**) as the Λ enantiomer.

*Quantum yields and lifetimes of [Ir(ppy)$_2$(**1**)]Cl*: The mixture of isomers (**A**) and (**B**) and the individual components behave similarly in air-equilibrated solution, with luminescence quantum yields close to 14 % (Tables 1 and 2). In deaerated conditions, however, we observed clear differences among the mixture and the isomers. The mixture has an intermediate quantum yield relative to the separated diastereoisomers; isomers (**A**) and (**B**) show lower and higher emission quantum yields, respectively (Table 2).

Table 2. Photophysical data for the separated diastereoisomers (**A**, Δ; **B**, Λ) and their mixture.[a]

Complex	λ_{exc} [nm][b]	Φ(air)	Φ(Ar)	τ(air) [ns]	τ(Ar) [ns]
[Ir(ppy)$_2$(**1**)]Cl mixture	380	0.14	0.54	690	2800
[Ir(ppy)$_2$(**1**)]Cl isomer (**A**)	380	0.13	0.49	670	2700
[Ir(ppy)$_2$(**1**)]Cl isomer (**B**)	380	0.14	0.70	680	2900

[a] The solutions were measured in air-equilibrated solvent (air) and in argon-saturated solvent degassed by bubbling argon through it for 20–30 min (Ar). [b] The optical density at the excitation wavelength was kept below 0.1.

As we discussed in the previous section, the substitution of an aliphatic system with the βCD results in a long extension of the lifetime and a large increase in emission quantum yields.

We have speculated that such an effect could be due to a noncovalent interaction of the ppy ligands coordinated to the Ir with the hydrophobic cavity of the covalently attached βCD. Indeed, it is known that CD can act simultaneously as both a first- and a second-sphere ligand when covalently attached to a potential guest.[10] This can enhance the photophysical properties of the guest mainly in three ways, by: a) limiting the molecular degrees of freedom of the chemical bonds, thus reducing the nonradiative deactivation of the triplet excited state; b) changing the microenvironmental polarity; c) preventing the excited-state quenching from dynamic collision or oxygen energy transfer.

The observed changes in guest phosphorescence in the presence of CD provide clear evidence that the inclusion complex has formed but they give limited structural information on the geometry and mode of inclusion. More data can be obtained from molecular modeling based on NMR studies, which can show specific interactions between specific parts of the guest and host. Inspection of a molecular model (not shown) of our system reveals that a hydrophobic pocket is formed on the primary side of the cavity due to the methylation of the hydroxyl groups. Moreover, the metal complex with the cyclodextrin appended is forced to be close to this substituted rim because the covalent link is relatively short. Preliminary high-resolution NMR investigations (not shown) on the **A** (Δ) diastereoisomer show that there is interaction between the iridium complex and the primary side of the attached CD. The rather large size of the Ir complex as compared with the diameter of the βCD cavity would not allow the formation of a real inclusion complex but instead give only a "semi-inclusion" complex of, for example, the aromatic ligands. A full account giving the assignments and analyzing the ROESY (rotating-frame Overhauser effect spectroscopy) contacts in terms of a 3D structure will be given elsewhere.

An additional effect of the βCD is the large and unexpected difference in the quantum yields of the two diastereoisomeric forms of the complex [Ir(ppy)$_2$(**1**)]Cl (Table 2). This can be explained by a preferential interaction of the chiral βCD with one of the enantiomers of the attached metal complex. The inherent chirality of the octahedral trisbidentate complex (Figure 5) is recognized by the cyclodextrin and probably leads to a stronger or deeper interaction in the case of one diastereoisomer than of the other. A macroworld analogy to describe the effect of semi-inclusion, which is different for the diastereoisomers, is to consider the pair of enantiomeric Ir complexes as chiral "heads" which each put on the same enantiopure cyclodextrin as a chiral "hat"; the interactions between the heads and the hat are different, and result in different effects of the hat on the properties of the head. This idea is corroborated by the example of chiral recognition of helical metal complexes by CDs reported by Kano,[66] who has investigated the interaction of the Ru(phen)$_3$ in water with CDs fully carboxylated on their primary side.

Conclusions

We have described the design and preparation, by "click chemistry," of novel Ru and Ir complexes with the cyclodextrin-, methyl-, and adamantane-appended triazole-pyridine ligands pytl-CD, pytl-Me, and pytl-ada. The preparations of the heteroleptic complexes of Ru and Ir with bipyridine (bpy) and phenyl-pyridine (ppy), respectively, resulting in $[Ru(bpy)_2(pytl-R)]Cl_2$, and $[Ir(ppy)_2(pytl-R)]Cl$ are described. The two diastereoisomeric forms of the Ir complex of a cyclodextrin-appended ligand $[Ir(ppy)_2(\mathbf{1})]Cl$ were separated by HPLC and characterized by NMR and circular dichroism spectroscopy. The luminescence of the Ru complexes (at 610–615 nm upon excitation at 448 or 420 nm) has a low quantum yield (0.005–0.006) and short lifetime (20–30 ns) and is not affected by oxygen. In contrast, the presence of the pytl ligand in the cyclometalated Ir complexes gives a series of highly luminescent compounds with emission quantum yields ranging between 0.23 and 0.70. Interestingly, it was found that the nature of the substituent strongly affects Φ and τ values of such complexes; the emission intensity is enhanced on going from the adamantane-appended ($[Ir(ppy)_2(\mathbf{2})]Cl$ to the cyclodextrin-appended derivative $[Ir(ppy)_2(\mathbf{1})]Cl$. The luminescence enhancement is observed both in argon-saturated and in air-equilibrated water solutions. Large differences between the quantum yields of the two diastereoisomers (**A**, Δ) and (**B**, Λ) of $[Ir(ppy)_2(\mathbf{1})]Cl$ were observed also. These effects are ascribed to a partial self-inclusion of the Ir complex into the primary side of the chiral βCD cavity, which acts as an enantioselective second-sphere ligand. This limits the vibration modes of the ligands, changes the micropolarity around the emissive excited state, and shields it from a quencher such as oxygen. The excited state of the Ir complexes is an admixture of ^3MC and ^3MLCT states and it is mainly ligand (ppy)-based. The phenyl and the pyridine moieties of the ppy ligand are expected to contribute most to the HOMO and LUMO of the complex, respectively. This was also confirmed by studies on $Ir(F_2ppy)_2(\mathbf{2})]Cl$, in which the introduction of fluorine on the phenyl rings produces bright blue emitting compounds (450 nm), because it lowers the energy of the HOMO orbital.

These new ligands for highly luminescent iridium complexes can be prepared easily by click chemistry, and the luminescence wavelength and intensity can be tuned by introducing substituents on the ppy or appending a cyclodextrin, respectively. In particular, the presence of the β-cyclodextrin leads to species that are also highly luminescent in air-equilibrated water solutions, by reducing the sensitivity of the Ir complexes to dioxygen. This opens new horizons for the preparation and application of new luminescent iridium complexes, for example, in electrochemiluminescent devices with highly improved efficiency.

Experimental Section

General: THF was purified by distillation under nitrogen from sodium/benzophenone, and dry DMF was purchased from Fluka. The "magic mixture" eluent was a mixture of H_2O (300 mL), NaCl (30 g), acetonitrile (1200 mL), and MeOH (300 mL). Compounds **4a**, **4b**, and **5**, and the Ir^{III} μ-chloro-bridged dimers $(ppy)_2Ir(\mu\text{-}Cl)_2Ir(ppy)_2$, and $(F_2ppy)_2Ir(\mu\text{-}Cl)_2Ir(F_2ppy)_2$, were prepared according to literature procedures.[42,67] All other chemicals were purchased from Aldrich, Fluka, or Acros and were used as received. Analytical TLC was performed on Merck precoated silica gel 60 F-254 plates (layer thickness 0.25 mm) and the compounds were visualized by UV irradiation at $\lambda = 254$ nm and/or $\lambda = 366$ nm and by staining with phosphomolybdic acid reagent or $KMnO_4$. Purifications by silica gel chromatography were performed using Acros (0.035–0.070 mm, pore diameter ≈ 6 nm) silica gel. All click reactions were performed in an oxygen-free atmosphere of N_2 by using Schlenk conditions and distilled solvents.

NMR: ^1H NMR spectra reported in the Supporting Information were recorded, at 25°C, on a Varian Inova 400 or a Bruker DMX-300 machine operating at 400 or 300 MHz, respectively. ^{13}C NMR spectra were recorded on a Bruker DMX-300 machine operating at 75 MHz. ^1H NMR chemical shifts (δ) are reported in parts per million (ppm) relative to a residual proton peak of the solvent: $\delta = 3.31$ for CD_3OD, $\delta = 7.26$ for $CDCl_3$, and $\delta = 2.50$ for DMSO. Multiplicities are reported as: s (singlet), d (doublet), t (triplet), q (quartet), dd (doublet of doublets), ddd (doublet of doublet of doublets), dt (doublet of triplets), or m (multiplet). Broad peaks are indicated by b. Coupling constants are reported as a J value in Hertz (Hz). The number of protons (n) for a given resonance is indicated as nH, and is based on spectral integration values. ^{13}C NMR chemical shifts (δ) are reported in ppm relative to a residual carbon peak of the solvent: $\delta = 49.0$ for CD_3OD, $\delta = 77$ for $CDCl_3$ and $\delta = 40$ for DMSO.

Mass spectrometry: High-resolution MS measurements were performed on a JEOL AccuTOF instrument (ESI) with water or methanol as the solvent.

High-performance liquid chromatography: HPLC was carried out on a Shimadzu LC-20AT HPLC system equipped with a UV/Vis detector SPD-10AV and a fraction collector. Columns were purchased from Dr. Maisch GmbH. The purity of the compounds was tested by analytical HPLC. A solution (20 μL) was injected into a ReproSil 100 C18 column (3 μm; 150 mm × 3 mm), operating at 30 °C. The detection wavelengths were fixed at 254 and 215 nm. A gradient of H_2O and acetonitrile both containing 0.1 % v/v TFA was used as mobile phase, with a flow rate of 0.4 mL min^{-1}. The compounds were purified on a milligram scale by means of semipreparative HPLC. A solution (2 mL) was injected into a ReproSil 100 C8 column (5 μm; 250 mm × 10 mm) operating at 30 °C. The detection wavelengths were fixed at 254 and 215 nm. A gradient of H_2O and acetonitrile both containing 0.1 % v/v HCl was used as mobile phase, with a flow rate of 4 mL min^{-1}. In this case HCl was used to ensure that the chloride was the only counterion of the isolated compounds. In all cases the samples were prepared by dissolving the compound in H_2O/acetonitrile mixtures (95:5 or 1:1 v/v), and filtered on a nylon syringe filter (0.2 μm).

X-ray crystallography: An $[Ir(ppy)_2(\mathbf{2})]Cl$ single crystal was grown by slow diffusion of diethyl ether into a solution of the pure compound in chloroform. Single crystals of **2** and **3** were grown by slow evaporation of a solution of the respective compound in diethyl ether/heptane. The crystal data and summaries of the data collection and structure refinement are given in Table S1, and selected distances and bond angles are in Tables S2–S4. The atomic coordinates and equivalent isotropic displacement parameters for the non-hydrogen atoms are given in Tables S5–S7. All measurements were performed at −65 °C. The structures of **2** and **3** were solved by the CRUNCH program.[68] All non-hydrogen atoms were refined with anisotropic temperature factors. The hydrogen atoms were placed at calculated positions, and refined isotropically in riding mode.

The structure of $[Ir(ppy)_2(pytl\text{-}ada)]Cl$ ($[Ir(ppy)_2(\mathbf{2})]Cl$) was solved by the PATTY option[69] of the DIRDIF program system.[70] Despite the presence of rather heavy atoms in this compound no reliable data could be collected above $\theta = 25°$. However, the internal consistency of the data is adequate ($R_{int} = 0.037$). Almost all non-hydrogen atoms were refined with anisotropic temperature factors. These hydrogen atoms were placed at calculated positions, and refined isotropically in riding mode. However, no hydrogen atoms could be found for the water molecule O1, probably because of the rather large anisotropic thermal displacement parameters of O1. As a consequence, no possible hydrogen bonds could be determined. The assignment of carbon to atoms C33 and C45 and of nitrogen to atoms N22 and N34 is based on the refinement of the occupancy factors for these atoms, the clear presence of hydrogen atoms near C33 and C45 in the difference Fourier map, and the absence of any such indications near N22 and N34. A few atoms, notably C14, C15, C16, and C19, have rather pronounced anisotropic thermal displacement parameters, indicating a slight positional disorder. Parameterization of this disorder proved impossible because it resulted in physically unacceptable values.

CCDC MFLADA 699148 (**2**), MFLIGA 699149 (**3**) and FELIC1 699147 ([Ir(ppy)$_2$(**2**)]Cl) contain the supplementary crystallographic data for this paper. These data can be obtained free of charge from The Cambridge Crystallographic Data Centre via www.ccdc.cam.ac.uk/data_request/cif.

Circular dichroism: Circular dichroism spectra were recorded on a Jasco 810 spectropolarimeter equipped with a Jasco PTC-423S/L Peltier-type temperature control unit, and were measured in MilliQ water at 20 °C.

Emission: Steady-state emission spectra were recorded on a HORIBA Jobin Yvon IBH FL-322 Fluorolog 3 spectrometer equipped with a 450 W xenon arc lamp, double-grating excitation and emission monochromators (2.1 nm mm^{-1} dispersion; 1200 grooves mm^{-1}), and a TBX-4-X single-photon-counting detector. Emission spectra were corrected for source intensity (lamp and grating) and emission spectral response (detector and grating) by standard correction curves. Luminescence quantum yields (Φ_{em}) were measured in optically dilute solutions (O.D. < 0.1 at excitation wavelength), using [Ru(bpy)$_3$]Cl$_2$ in aerated H$_2$O (Φ_{em} = 0.028) or diphenylanthracene in cyclohexane (Φ_{em} = 0.9) as reference.

Time-resolved measurements up to ~5 μs were performed using the time-correlated single-photon-counting (TCSPC) option on the Fluorolog 3. Nano-LEDs (295 or 431 nm; FWHM < 750 ps) with repetition rates between 10 kHz and 1 MHz were used to excite the sample. The excitation sources were mounted directly on the sample chamber at 90 °C of a double-grating emission monochromator (2.1 nm mm^{-1} dispersion; 1200 grooves mm^{-1}) and collected by a TBX-4-X single-photon-counting detector. The photons collected at the detector are correlated by a time-to-amplitude converter (TAC) to the excitation pulse. Signals were collected using an IBH DataStation Hub photon-counting module and data was analyzed by the commercially available DAS6 software (HORIBA Jobin Yvon IBH). The goodness of fit was assessed by minimizing the reduced chi-squared function (χ^2) and visual inspection of the weighted residuals.

Nanosecond transient spectroscopy: For nanosecond transient absorption spectra, a sample with optical density of around 0.8 at the excitation wavelength (500 nm) was excited with a laser pulse from a master-oscillator power oscillator (MOPO) pumped by a Q-switched beam locked Nd:YAG laser with a 10 ns pulse width and 10 Hz repetition rate. The excited-state absorption was probed by using a Xe flash lamp with the same repetition rate. The pulse energy was 2 mJ pulse^{-1}. The signal was recorded with a CCD camera as the detector. The excited-state spectra were obtained from $\Delta A = \log(I/I0)$. The spectra were processed on an in-house Lab View program.

Acknowledgements

The authors thank the European Union for support through the Marie Curie Research and Training Network UNI-NANOCUPS. M.F. acknowledges the University "La Sapienza" of Rome for a scholarship. Y.V. acknowledges the Fundación Ramón Areces for financial support. R.J.M.N. acknowledges the Royal Netherlands Academy of Science and Art for financial support.

---

[1] H. C. Kolb, M. G. Finn, K. B. Sharpless, *Angew. Chem.* **2001**, *113*, 2056–2075; *Angew. Chem. Int. Ed.* **2001**, *40*, 2004–2021.
[2] We prefer the designation pytl for the 2-(1-substituted-1*H*-1,2,3-triazol-4-yl)pyridine ligand rather than pyta coined by Obata et al. Ref [5], because the latter is already in use for 4-pyridylthioacetate: M. Kondo, M. Miyazawa, Y. Irie, R. Shinagawa, T. Horiba, A. Nakamura, T. Naito, K. Maeda, S. Utsuno, F. Uchida, *Chem. Commun.* **2002**, 2156–2157.
[3] D. J. V. C. van Steenis, O. R. P. David, G. P. F. van Strijdonck, J. H. van Maarseveen, J. N. H. Reek, *Chem. Commun.* **2005**, 4333–4335.
[4] D. Schweinfurth, K. I. Hardcastle, U. H. F. Bunz, *Chem. Commun.* **2008**, 2203–2205.
[5] M. Obata, A. Kitamura, A. Mori, C. Kameyama, J. A. Czaplewska, R. Tanaka, I. Kinoshita, T. Kusumoto, H. Hashimoto, M. Harada, Y. Mikata, T. Funabiki, S. Yano, *Dalton Trans.* **2008**, 3292–3300.
[6] O. David, S. Maisonneuve, J. Xie, *Tetrahedron Lett.* **2007**, *48*, 6527–6530.
[7] J. Szejtli, *Chem. Rev.* **1998**, *98*, 1743–1754.
[8] G. Wenz, *Angew. Chem.* **1994**, *106*, 851–870; *Angew. Chem. Int. Ed. Engl.* **1994**, *33*, 803–822.
[9] G. Wenz, B. H. Han, A. Müller, *Chem. Rev.* **2006**, *106*, 782–817.
[10] F. Hapiot, S. Tilloy, E. Monflier, *Chem. Rev.* **2006**, *106*, 767–781.
[11] H. Dodziuk, *Cyclodextrin and Their Complexes: Chemistry, Analytical Methods, Applications* (Ed.: H. Dodziuk), Wiley-VCH, Weinheim, **2006**.
[12] R. Breslow, S. D. Dong, *Chem. Rev.* **1998**, *98*, 1997–2011.
[13] A. Douhal, *Cyclodextrin Materials Photochemistry, Photophysics and Photobiology, Vol. 1* (Ed.: A. Douhal), Elsevier, Amsterdam, **2006**.
[14] J. M. Haider, R. M. Williams, L. De Cola, Z. Pikramenou, *Angew. Chem.* **2003**, *115*, 1874–1877; *Angew. Chem. Int. Ed.* **2003**, *42*, 1830–1833.
[15] J. M. Haider, Z. Pikramenou, *Chem. Soc. Rev.* **2005**, *34*, 120–132.
[16] H. F. M. Nelissen, M. Kercher, L. De Cola, M. C. Feiters, R. J. M. Nolte, *Chem. Eur. J.* **2002**, *8*, 5407–5414.
[17] J. A. Faiz, R. M. Williams, M. J. J. P. Silva, L. De Cola, Z. Pikramenou, *J. Am. Chem. Soc.* **2006**, *128*, 4520–4521.
[18] W. Xu, A. Jain, B. A. Betts, J. N. Demas, B. A. DeGraff, *J. Phys. Chem. A* **2002**, *106*, 251–257.
[19] D. Beck, J. Brewer, J. Lee, D. McGraw, B. A. DeGraff, J. N. Demas, *Coord. Chem. Rev.* **2007**, *251*, 546–553.
[20] M. Felici, P. Contreras, R. M. Williams, Y. Vida, E. Orselli, L. De Cola, M. C. Feiters, R. J. M. Nolte, *Proceedings on the 7th Netherlands Catalysis and Chemistry Conference*, **2007**, pp. 194.
[21] S. Welter, N. Salluce, P. Belser, M. Groeneveld, L. De Cola, *Coord. Chem. Rev.* **2005**, *249*, 1360–1371.
[22] O. Bossart, L. De Cola, S. Welter, G. Calzaferri, *Chem. Eur. J.* **2004**, *10*, 5771–5775.
[23] S. Welter, K. Brunner, J. W. Hofstraat, L. De Cola, *Nature* **2003**, *421*, 54–57.
[24] L. De Cola, P. Belser, A. von Zelewsky, F. Vogtle, *Inorg. Chim. Acta* **2007**, *360*, 775–784.
[25] M. W. Cooke, G. S. Hanan, F. Loiseau, S. Campagna, M. Watanabe, Y. Tanaka, *J. Am. Chem. Soc.* **2007**, *129*, 10479–10488.
[26] A. Juris, V. Balzani, F. Barigelletti, S. Campagna, P. Belser, A. Vonzelewsky, *Coord. Chem. Rev.* **1988**, *84*, 85–277.
[27] C. Dragonetti, S. Righetto, D. Roberto, R. Ugo, A. Valore, S. Fantacci, A. Sgamellotti, F. De Angelis, *Chem. Commun.* **2007**, 4116–4118.
[28] L. Flamigni, J. P. Collin, J. P. Sauvage, *Acc. Chem. Res.* **2008**, *41*, 857–871.
[29] L. Flamigni, A. Barbieri, C. Sabatini, B. Ventura, F. Barigelletti, *Top. Curr. Chem.* **2007**, *281*, 143–203.
[30] A. B. Tamayo, S. Garon, T. Sajoto, P. I. Djurovich, I. M. Tsyba, R. Bau, M. E. Thompson, *Inorg. Chem.* **2005**, *44*, 8723–8732.
[31] W. J. Finkenzeller, M. E. Thompson, H. Yersin, *Chem. Phys. Lett.* **2007**, *444*, 273–279.
[32] J. Li, P. I. Djurovich, B. D. Alleyne, M. Yousufuddin, N. N. Ho, J. C. Thomas, J. C. Peters, R. Bau, M. E. Thompson, *Inorg. Chem.* **2005**, *44*, 1713–1727.
[33] F. Lafolet, S. Welter, Z. Popović, L. D. Cola, *J. Mater. Chem.* **2005**, *15*, 2820–2828.

[34] A. B. Tamayo, B. D. Alleyne, P. I. Djurovich, S. Lamansky, I. Tsyba, N. N. Ho, R. Bau, M. E. Thompson, *J. Am. Chem. Soc.* **2003**, *125*, 7377–7387.
[35] P. Coppo, E. A. Plummer, L. De Cola, *Chem. Commun.* **2004**, 1774–1775.
[36] J. T. Fletcher, B. J. Bumgarner, N. D. Engels, D. A. Skoglund, *Organometallics* **2008**, *27*, 5430–5433.
[37] C. Richardson, C. M. Fitchett, F. R. Keene, P. J. Steel, *Dalton Trans.* **2008**, 2534–2537.
[38] Y. Li, J. C. Huffman, A. H. Flood, *Chem. Commun.* **2007**, 2692–2694.
[39] B. Schulze, C. Friebe, M. D. Hager, A. Winter, R. Hoogenboom, H. Görls, U. S. Schubert, *Dalton Trans.* **2009**, 787–794.
[40] E. Orselli, R. Q. Albuquerque, P. M. Fransen, R. Fröhlich, H. M. Janssen, L. De Cola, *J. Mater. Chem.* **2008**, *18*, 4579–4590.
[41] A. P. Croft, R. A. Bartsch, *Tetrahedron* **1983**, *39*, 1417–1474.
[42] M. Felici, M. Marzá-Pérez, N. S. Hatzakis, R. J. M. Nolte, M. C. Feiters, *Chem. Eur. J.* **2008**, *14*, 9914–9920.
[43] E. Orselli, G. S. Kottas, A. E. Konradsson, P. Coppo, R. Fröhlich, L. De Cola, A. van Dijken, M. Büchel, H. Börner, *Inorg. Chem.* **2007**, *46*, 11082–11093.
[44] P. J. Hay, *J. Phys. Chem. A* **2002**, *106*, 1634–1641.
[45] K. Dedeian, J. Shi, N. Shepherd, E. Forsythe, D. C. Morton, *Inorg. Chem.* **2005**, *44*, 4445–4447.
[46] R. Hage, J. G. Haasnoot, D. J. Stufkens, T. L. Snoeck, J. G. Vos, J. Reedijk, *Inorg. Chem.* **1989**, *28*, 1413–1414.
[47] M. Duati, S. Tasca, F. C. Lynch, H. Bohlen, J. G. Vos, S. Stagni, M. D. Ward, *Inorg. Chem.* **2003**, *42*, 8377–8384.
[48] T. E. Keyes, B. Evrard, J. G. Vos, C. Brady, J. J. McGarvey, P. Jayaweera, *Dalton Trans.* **2004**, 2341–2346.
[49] W. R. Browne, C. M. O'Connor, H. P. Hughes, R. Hage, O. Walter, M. Doering, J. F. Gallagher, J. G. Vos, *Dalton Trans.* **2002**, 4048–4054.
[50] R. Hage, J. G. Haasnoot, J. Reedijk, R. Wang, E. M. Ryan, J. G. Vos, A. L. Spek, A. J. M. Duisenberg, *Inorg. Chim. Acta* **1990**, *174*, 77–85.
[51] W. R. Browne, W. Henry, P. Passaniti, M. T. Gandolfi, R. Ballardini, C. M. O'Connor, C. Brady, C. G. Coates, J. G. Vos, J. J. McGarvey, *Photochem. Photobiol. Sci.* **2007**, *6*, 386–396.
[52] T. Sajoto, P. I. Djurovich, A. Tamayo, M. Yousufuddin, R. Bau, M. E. Thompson, R. J. Holmes, S. R. Forrest, *Inorg. Chem.* **2005**, *44*, 7992–8003.
[53] I. Avilov, P. Minoofar, J. Cornil, L. De Cola, *J. Am. Chem. Soc.* **2007**, *129*, 8247–8258.
[54] M. G. Colombo, H. U. Guedel, *Inorg. Chem.* **1993**, *32*, 3081–3087.
[55] G. F. Strouse, H. U. Guedel, V. Bertolasi, V. Ferretti, *Inorg. Chem.* **1995**, *34*, 5578–5587.
[56] F. W. M. Vanhelmont, H. U. Gudel, M. Fortsch, H. B. Burgi, *Inorg. Chem.* **1997**, *36*, 5512–5517.
[57] L. A. Sacksteder, M. Lee, J. N. Demas, B. A. Degraff, *J. Am. Chem. Soc.* **1993**, *115*, 8230–8238.
[58] P. I. Djurovich, D. Murphy, M. E. Thompson, B. Hernandez, R. Gao, P. L. Hunt, M. Selke, *Dalton Trans.* **2007**, 3763–3770.
[59] C. S. Mak, A. Hayer, S. I. Pascu, S. E. Watkins, A. B. Holmes, A. Köhler, R. H. Friend, *Chem. Commun.* **2005**, 4708–4710.
[60] L. J. Bellamy, The Infrared Spectra of complex molecules, Vol. 1, 3rd ed., (Ed.: L. J. Bellamy), Hastel Press, New York, **1975**, spectrum 13298.
[61] K. Ichimura, T. Kobayashi, K. A. King, R. J. Watts, *J. Phys. Chem.* **1987**, *91*, 6104–6106.
[62] M. A. Baldo, C. Adachi, S. R. Forrest, *Phys. Rev. B* **2000**, *62*, 10967–10977.
[63] C. Creutz, M. Chou, T. L. Netzel, M. Okumura, N. Sutin, *J. Am. Chem. Soc.* **1980**, *102*, 1309–1319.
[64] K. A. McGee, K. R. Mann, *Inorg. Chem.* **2007**, *46*, 7800–7809.
[65] F. J. Coughlin, M. S. Westrol, K. D. Oyler, N. Byrne, C. Kraml, E. Zysman-Colman, M. S. Lowry, S. Bernhard, *Inorg. Chem.* **2008**, *47*, 2039–2048.
[66] K. Kano, H. Hasegawa, *J. Am. Chem. Soc.* **2001**, *123*, 10616–10627.
[67] I. R. Laskar, S. F. Hsu, T. M. Chen, *Polyhedron* **2005**, *24*, 189–200.
[68] R. de Gelder, R. A. G. de Graaff, H. Schenk, *Acta Crystallogr. Sect. A* **1993**, *49*, 287–293.
[69] P. T. Beurskens, G. Beurskens, M. Strumpel, C. E. Nordman in *Patterson and Pattersons* (Eds.: J. P. Glusker, B. K. Patterson, M. Rossi), Clarendon Press, Oxford, **1987**, pp. 356–367.
[70] DIRDIF-96. A computer program system for crystal structure determination by Patterson methods and direct methods applied to difference structure factors, P. T. Beurskens, G. Beurskens, W. P. Bosman, R. de Gelder, S. Garcia-Granda, R. O. Gould, R. Israel, J. M. M. Smits, **1996**.

Received: June 10, 2009

Photophysics

M. Felici, P. Contreras-Carballada, Y. Vida, J. M. M. Smits, R. J. M. Nolte, L. De Cola, R. M. Williams,* M. C. Feiters** .... ■■■■–■■■■

Ir^{III} and Ru^{II} Complexes Containing Triazole-Pyridine Ligands: Luminescence Enhancement upon Substitution with β-Cyclodextrin

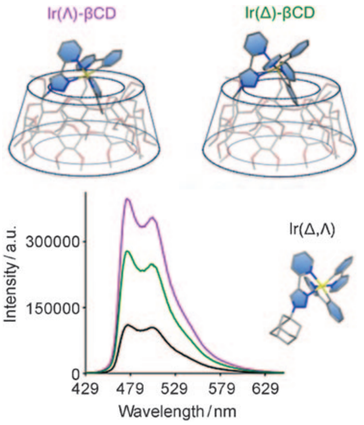

Brighter metal complexes: Ru and Ir complexes (illustrated) were prepared from novel triazole-pyridine (pytl) ligands obtained by "click chemistry." The photophysical properties of these complexes were even further enhanced when a β-cyclodextrin was attached to the pytl. Significant differences between the quantum yields of the Δ and Λ diastereoisomers of the Ir complex were attributed to different interactions with their chiral cyclodextrin substituents.